ANALYSIS ON VARIATION CHARACTERISTICS OF REMOTE SENSING REFLECTANCE AND ITS INFLUENCING FACTORS IN OIL-POLLUTED WATER

Miaofen Huang (1), Yang Liu(2), Xufeng Xing(1), Nannan Zhang (2), Zhonglin Wang (1)

[1] Guangdong Ocean University, No. 1 Haida Road, Mazhang District, Zhanjiang, 524088, China
[2] PetroChina Exploration & Development Research Institute, No. 20 Xueyuan Road, Haidian District, Beijing, 100083, China
Email: hmf808@163.com; liuyang_rs@petrochina.com.cn; 4918585@qq.com; 76190286@qq.com; wzllin@126.com

KEY WORDS: Oil-polluted water, Remote sensing reflectance, Spectral characteristics influencing factors

ABSTRACT: As a distribution center of crude oil and refined oil products, Dalian Port of China inevitably causes oil-pollution in water, becoming a good experimental area for the study of the influence of oil substances on the apparent optical characteristics of water. From August 25 to 27, 2018, the data of remote sensing reflectance, oil concentration, chlorophyll concentration, suspended matter concentration, Velocity and direction of flow were measured at three stations and 30 observation moments in the sea area of Dalian Port of China, as well as tidal data provided by the maritime service network. On the basis of comparing the influence characteristics of chlorophyll and suspended matter on remote sensing reflectance spectra, the spectral changes of apparent optical properties after superimposed oil material were analyzed. The results show that: (2) The observation time of each station is at different times of high and low tide, and the water flow direction and velocity are different, which leads to complex changes of oil concentration, chlorophyll concentration and suspended sediment concentration with time, leading to complex changes of normalized remote sensing reflectance. (2) The apparent optical properties have double peaks and single peaks, with the first peak at 560-570nm which is caused by the interaction of chlorophyll and oil substances and the second peak at 680nm which is caused by the fluorescence peak of chlorophyll-a.

1. INTRODUCTION

Remote sensing reflectance (Rrs) is the basic physical quantity that can be directly obtained by remote sensing of water color. It is the ratio of the incident radiation to the water-leaving radiance which is determined by the composition of water bodies. Different components of water bodies have different inherent optical properties (including absorption coefficient and scattering absorption), resulting in the difference in shape and magnitude of water-leaving radiance determined by the backscattering coefficient (Ma, et al., 2007; Lee& Carder, 2004; Jiang ,et al., 2019).

At present, the influencing factors of Rrs mainly focus on the three element of water color, namely yellow matter, chlorophyll and suspended matter. These factors lead to different spectral characteristics of Rrs (Cannizzaro & Carder,2006; Luba& Loise,2007; Catherine ,et al. ,2019;YIN ,et al. ,2011).Scholars have done a lot of work on the determination of the main water-color factors in case II water bodies to measure the inherent optical properties (absorption coefficient and backscattering) , such as chlorophyll, suspended sediment, yellow substances and pure water, many parameter models have been proposed (Pope & Fry, 1997; Smith & Baker, 1981; Gallegos & Murtha,1992 ; Yu, et al.,2003; Song, et al., 2006), It lays a foundation for understanding the influence of the three major components of ocean color on Rrs. In addition, remote sensing reflectance use empirical model, semi-empirical model and physical model to estimate the important physical quantities of water components, which has been studied and discussed by many scholars, and various models of extracting water components based on remote sensing reflectance have been constructed (Sławomir, et al.,2016; Martin, et al.,2017 ;Monika, et al.,2018 ; Zhang, et al.,2018; Chen, et al.,2014; Lyu, et al.,2013).

In the petroleum-polluted water, the existence of petroleum substance must affect Rrs to some extent. Researches on "apparent optical properties, inherent optical properties (absorption coefficient and scattering coefficient), fluorescence characteristics" of petroleum-polluted water have been carried out. (Huang, et al., 2016 & 2014a & 2014b & 2015), A separation model for the contribution of petroleum and suspended matter to backscattering coefficient is established successfully (Huang, et al, 2017). At the same time, an algorithm for inversion of petroleum concentration in water bodies by using inherent optical properties and apparent optical properties have been determined (Huang, et al., 2012&2015). However, existing models mainly focus on single element, and the research on Rrs is mainly limited to petroleum wastewater, which weakens the applicability of

inversion model, and studies on Rrs spectral characteristics of water bodies in natural water bodies are rarely reported.

In this paper, the Rrs, petroleum concentration, chlorophyll concentration, suspended matter concentration, velocity and flow direction and other measured data in the sea area of Dalian Port of China from August 25 to 27, 2018 were used to study the change characteristics of the Rrs of water, and further analyze the influencing factors

2. METHOD

2.1 Study Area and Site Distribution

The test site is located in Dagushan petrochemical district, Dalian Port, Liaoning province, China. The main petrochemical enterprises are west Pacific petrochemical company (xitai), YiShanda petrochemical co., LTD., Fujia petrochemical company, Dalian Port oil terminal, and Dalian LNG terminal of KunLun energy. Petrochemical production and tanker transportation inevitably bring petroleum pollution, which makes Dalian Port become the natural test base for studying the optical characteristics of petroleum-polluted water and the variation characteristics of petroleum concentration.

Three test sites were selected in Dalian Port, named as A, B and C respectively. Site A which water depth is 21.5 m on July 16, 2010 oil pipeline explosion has occurred, the sea bottom of the adsorption of crude oil into blocks of linoleum with a sunken bottom. During the observation period, typhoon “wenbiya” happened to pass through Dalian city, and the wild waves stirred up the oil substance on the sea floor. After the stirring, the water would be affected by oil. In addition, the hot weather and high water temperature would cause the oil lump on the bottom of the bottom to evaporate, making the water body oily. Site B is located in the channel of Dalian Port which water depth is 24.8 m, and the changes of petroleum concentration in the water bodies passing by the ship have a great impact. Site C which the water depth is 33.0 m is located on the east side of the island. Compared with the previous two sites the frequency of ships passing through this site is small and the disturbance caused by ships is small.

And the corresponding observation dates are from 7:00 to 17:00 on August 25, 26 and 27, 2018. The samples were numbered according to the station number and time, so the sample number was composed of the station number and time number. The time number was recorded as 1 to 11 from 7:00 to 17:00. The naming rules of the corresponding sites are: A1~A11, B1~B11, C1~ C1, where A1, B1 and C1 correspond to the observation time of 7:00, A2, B2 and C2 correspond to the observation time of 8:00. The rest can be done in the same manner .Due to the limitation of measurement time, the measurement time of some elements is 8:00, 10:00, 12:00, 14:00 and 16:00. Therefore, this paper mainly analyzes the data of these five observation times.

2.2 Field Data Collection and Method Description

The TD-500D Fluorescence Oil Meter (made by Turner Designs Hydrocarbon Instruments, Inc, USA), was used to determine petroleum concentration in water, the measuring principle of which is the molecular fluorescence spectrometric method, meeting *The Specification For Marine Monitoring-Part 4: Seawater Analysis(GB 17378.4-2007)* and The Water Quality Determination Of Petroleum Oil-Molecular Fluorescence Spectrometric Method(SL 366-2006).Before the instrument is used for measurement, it is necessary to calibrate the solid standard sample of the equipment by preparing the standard oil sample of n-hexane and petroleum standard substances, and then calibrate the solid standard sample in the field. The oil samples came from The China National Marine Environment Monitoring Center.

Chlorophyll-a (chl-a) is measured according to *The Marine monitoring -- part 7: ecological investigation and biological monitoring of offshore* (*GB 17378.7-2007) pollution* and spectrophotometric method is adopted. The spectrophotometer used is Shanghai spectral SP-752.

The suspended substance is measured in accordance with The national standard *Marine monitoring specifications part 4: seawater analysis (GB/T 17378.4-2007).* The instruments required for the measurement process include vacuum pump, extraction filter, balance, water sampler, measuring cylinder, filter membrane, filter membrane box, etc.

The above - water method is used for spectral measurement of water body. The measuring instrument is ASD FieldSpec3 3 50~2500nm, and the reference plate is the standard plate with 30% reflectivity.

The current meter used to measure flow velocity and direction is the type of SLC9-2DV. The depth of draft of the survey ship is 3 m. In order to ensure data quality, the depth of current meter is 6 m.
There is no tidal observation station in the study area in this paper, and there is no corresponding tidal measuring device during the test, so the tidal data provided by the China Oceanic Information Network.

2.3 Satellite Data

Landsat 8 satellite data used in this paper is from the satellite's official data released at https://earthexplorer.usgs.gov/. Landsat 8 is equipped with the Operational Land Imager (OLI), which is equipped with 9 operational land imager bands in visible near-infrared and short-wave infrared. Specific technical parameters are shown in Table 1.

Table 1 Specific technical parameters of Landsat8/ OLI

Band set	Spatial resolution	Orbital period/revisit period	Declare
B1: 433 – 453nm B2: 450 – 515nm B3: 525 – 600nm B4: 630 – 680nm B5: 845 – 885nm B6 SWIR1: 1570-1650nm B7 SWIR2: 2110-2290nm B9: 1360-1380nm	30 m	16day	Band 9 is set specifically for atmospheric correction

3. RESULTS AND DISCUSSION

3.1 Analysis of Environmental Factors in Dalian Port

3.1.1 Characteristics of Tidal and Flow Velocity Changes: Figure 1 shows the tidal change process during the observation period. The analysis of fig. 1 shows that during the observation period from 7 to 17 o 'clock, the three days are basically at a complete ebb tide, with the high tide around 10 o 'clock and the low tide around 16 o 'clock. Therefore, the tidal changes of the same observation site are different at different observation times. The incoming and outgoing tides are different, and the composition of seawater is also different.

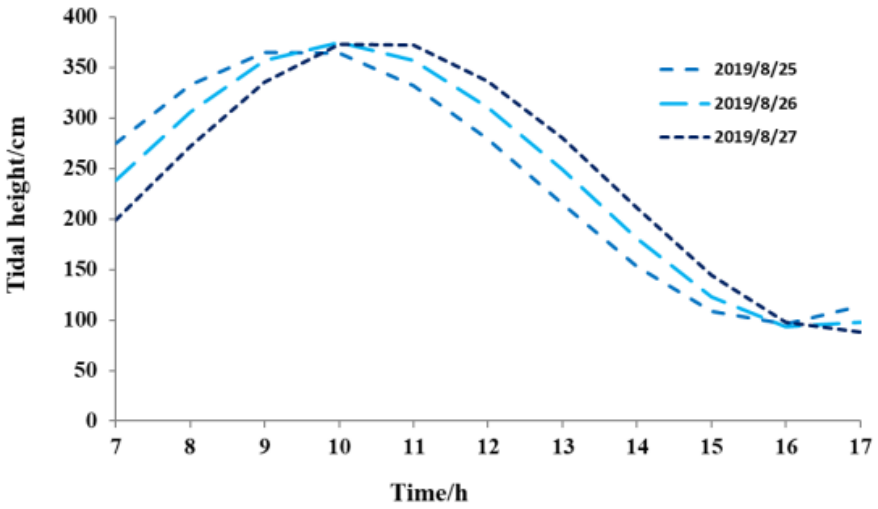

Fig.1 Tidal table in Dalian Port (Based on tidal datum, it is 190cm below sea level)

Figure 2 shows the flow rate and direction during the observation period. In the figure, 0° indicates the due north direction, the length of the line indicates the flow rate, and the direction of the arrow indicates the flow direction.

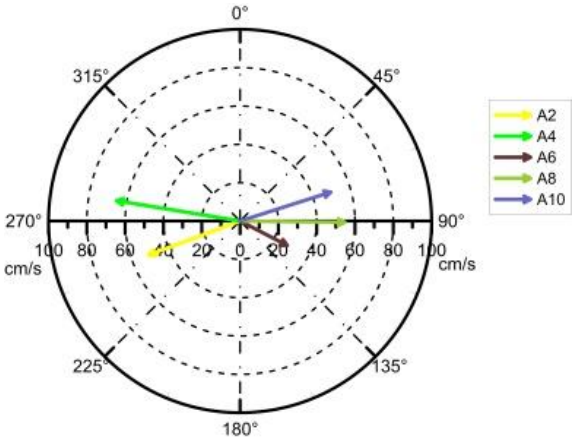

(a) Site A

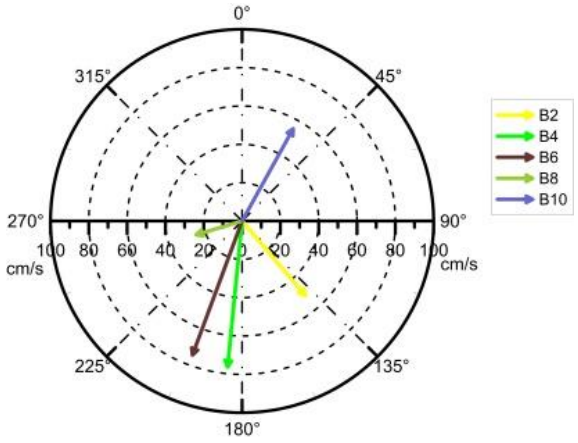

(b) Site B

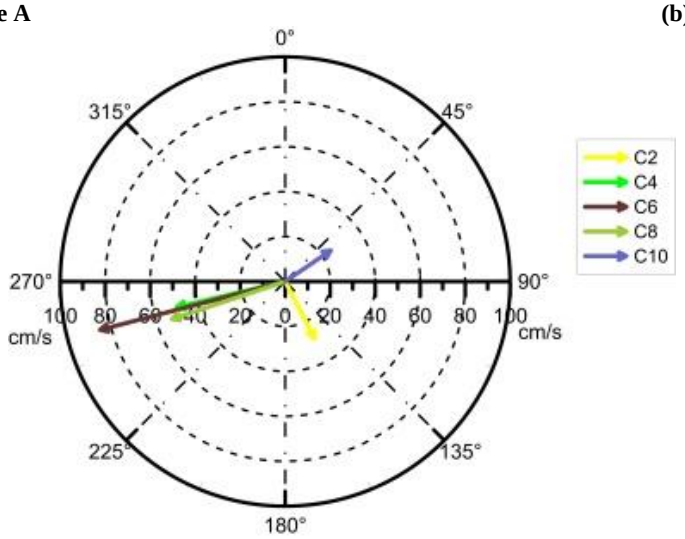

(c) Site C

Fig.2 Flow velocity and direction (observation depth in 6m)

It can be seen from figure 2 that all stations were at different ebb moments, with different ocean current direction and velocity. Site A is obviously affected by tides, with the rising tide in the west and the falling tide in the east and its velocity is between 27 and 65 cm/s. The high tide at site B is southeast flow, and the low tide is southwest flow. Generally speaking, the south flow is dominant. Site B is located on the shipping road, and the measurement of sea current is greatly affected by passing ships, with a velocity between 22 and 75 cm/s. Site C is located in the east direction of the island, and the channel formed between the two islands has a certain degree of influence on the sea current. Generally speaking, it flows southward at high tide and westwards at low tide. The velocity is between 21 and 85 cm/s.

3.1.2 Component Concentration Analysis: Figure 3 shows the change curve of suspension concentration with time at different observation times at three stations. It can be seen from figure 3 that among the three sites, the concentration of suspended substances in site A is the highest. At the climax point (10:00), the concentration reaches the highest value (7.6mg/L), and then gradually decreases. At 8:00 and 10:00, it is high tide, and the sea water comes mainly to the east, bringing more suspended substances from the bay. Later, it is low tide, and the sea water comes to the west, bringing less suspended substances in the sea water. The second is station B. No matter it is high tide or low tide, the change range is not big, basically stable between 2.3 and 3.3mg/L, and the maximum value occurs at 16:00. At this time, it is northward flow, and the sea water comes from the south, bringing more suspended objects. The smallest station is station C, which has a small range of change and basically stable between 1.3 and 2.0 mg/L. In general, there is little change in the suspended substance concentration.

Figure 4 shows the change curve of chlorophyll concentration with time at different observation times at the three sites. It can be seen from Fig. 4 that the chlorophyll concentration gradually decreases at high tide of site A and site B, and gradually increases at low tide, and reaches the highest value at low tide, in which the

chlorophyll concentration reaches 4.7mg/L at site A and 9.3mg/L at site B. The change trend of site C is contrary to that of the previous two sites. The chlorophyll concentration gradually increases at high tide, and decreases rapidly at low tide. When tide approaches the lowest tide, the chlorophyll reaches the lowest value at all observation time, which is 1.2mg/L. According to the flow chart, changes in chlorophyll concentration are also closely related to tidal changes, which is consistent with the research results of Xing, et al. (2018).

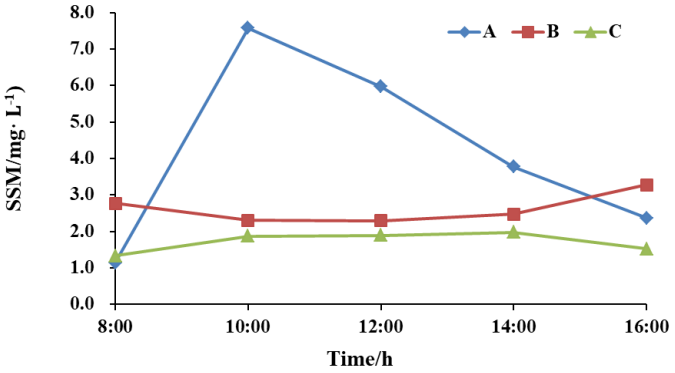

Fig. 3 The change curve of suspension concentration with time

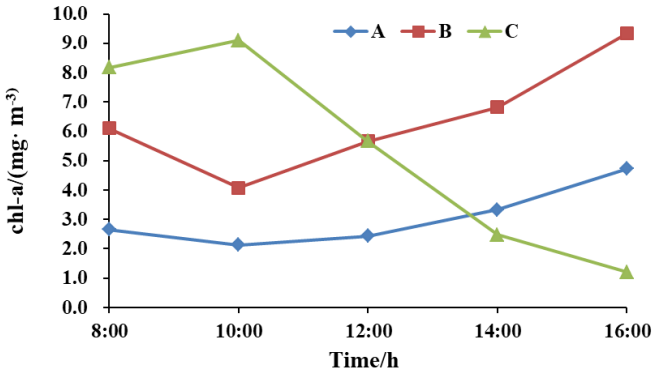

Fig. 4 The change curve of chlorophyll concentration with time

Figure 5 shows the change curve of petroleum concentration with time at different observation times at three stations. It can be seen from the figure that petroleum concentration changes with time in a complex manner, which is mainly affected by tidal changes. At different ebb and flow moments, different water flows lead to different oil content; The petroleum concentration of the site A shows decreasing trend at the moment of high tide, Indicating that the amount of petroleum coming to sea water at high tide is small, or from the east the external sea water will dilute the petroleum concentration of the station itself. The ebb tide later tends to have high petroleum coming from the west brings high petroleum concentration, resulting in a significant increase in petroleum concentration. But site C after 12:00 appeared a steep drop, this is mainly the ebb tide, for the west flow, sea water from the sea, plus this area away from the influence of oil sewage, so the petroleum concentration is relatively low. According to the variation value of the concentration, the petroleum concentration of site A ranged from 0.7 to 4.1 mg/L, site B from 1.0 to 9.3 mg/L, and site C from 0.2 to 7.8 mg/L. Among the three observation stations, the petroleum concentration of site B was in high state throughout the day.

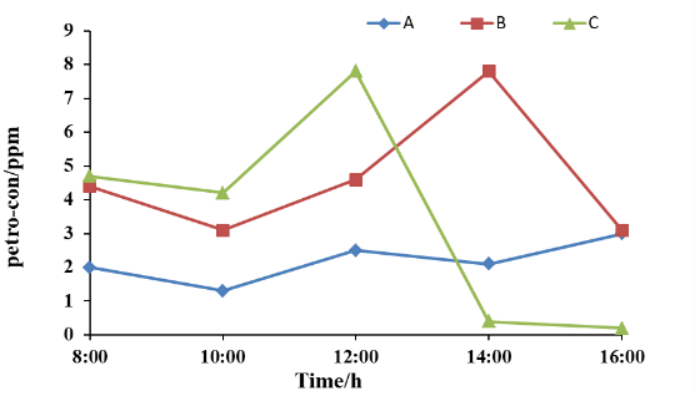

Fig. 5 The change curve of petroleum concentration with time

In conclusion, the observation time of each station is at different times of high tide and low tide, and the flow direction and velocity of water are different, resulting in complex changes of oil content, chlorophyll content and suspended matter content with time.

3.2 Spectral Characteristics of Rrs in Petroleum-polluted Water

A large number of studies have shown that the remote sensing reflectance is affected by inorganic suspended sediment, and a reflection peak will appear at 650-750nm. With the change of inorganic suspended sediment content, the width and height of this reflection peak will change significantly (Han,et al.,1994).
The curve of Rrs with chlorophyll concentration also has obvious characteristics. Affected by chlorophyll, the spectral curves of Rrs show reflectivity troughs near 440nm, reflectivity peaks near 470nm, and shoulder troughs formed by absorption of algal albumin near 630nm (shu, et al., 2000); There was an obvious fluorescence peak near 685nm, and the maximum growth rate was also at the position of fluorescence peak 685nm.

Figure 6 (a) - (d) shows the Rrs spectrum curve of petroleum-polluted water measured in the sea area of Dalian Port. By analyzing figure 6, it can be found that the variation characteristics of remote sensing reflection ratio spectrum curve can be divided into bimodal and unimodal types, in which the first peak value of bimodal type is 560-570nm and the second peak value is 680nm. The peak of single peak type is 560-570nm. The samples of A4, A6 and A8 belong to the single-peak type. Due to the low chlorophyll concentration content of these three sites, the fluorescence peak of 680nm did not appear. All the other samples showed fluorescence spikes. The content of chlorophyll in the sample of A10, B10 and C2 was higher than that in other samples, so the fluorescence peak at 680nm was higher than that in other samples. As can be seen from figure 3, in this experiment, the concentration of suspended matter is relatively low, so there is no obvious reflection peak at 650-750nm, and the peak at 560-570nm is not entirely due to chlorophyll, which is obviously closely related to oil. In other words, in oily water, the Rrs will show a significant peak in the range of 560-570nm.

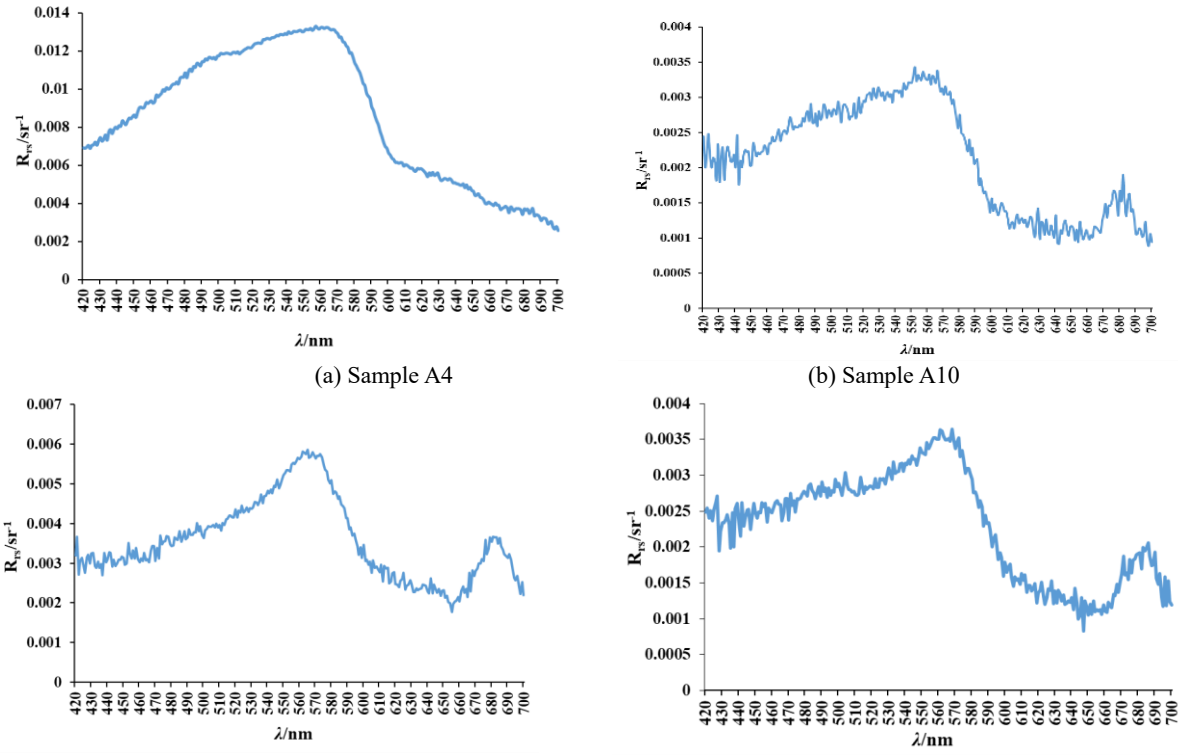

(a) Sample A4 (b) Sample A10

(c) Sample B10 (d) Sample C2

Fig. 6 The Rrs spectrum curve of petroleum-polluted water measured in the sea area of Dalian port

4. CONCLUSIONS

Because of the different components and their contents, the absorption and scattering of water body change, which makes the reflectivity of certain wavelength range significantly different. The influence of oil concentration, chlorophyll concentration, suspended matter concentration, velocity and flow direction and tidal

data on remote sensing reflectance is analyzed by using the measured data, which is helpful to separate the influence of oil substance on remote sensing reflectance.

However, in order to truly obtain the influence of oil substance on remote sensing reflectance, it is necessary to further analyze the influence of single element on remote sensing reflectance. On this basis, different components are combined to obtain the influence of comprehensive elements on remote sensing reflectance. The current radiation transfer mode Hydrolight provides a good platform for related research.

The conclusion obtained in this paper is that the remote sensing reflectance will show an obvious peak value at 560-570nm in oily water. Hydrolight software is needed to simulate the remote sensing reflectzance at different petroleum concentrations to further determine and explain, and determine the change characteristics of remote sensing reflectance at different oil concentration from the perspective of forward modeling.

ACKNOWLEDGMENT

This work was funded by National Natural Science Foundation of China under contract No. 41771384 , National Key Research and Development Projects under contract No. 2016YFC1401203, Provincial Special Funds for Economic Development (use of marine economic development) in 2018 under contract No.GDME-2018E003, Project of Enhancing School with Innovation of Guangdong Ocean University under contract No.GDOU2017052501 and Program for Scientific Research Start-up Funds of Guangdong Ocean University under contract No.E16187.

REFERENCES

Cannizzaro J. P. Carder K. L. 2006.Estimating chlorophyll a concentrations from remote-sensing reflectance in optically shallow waters. Remote Sensing of Environment, pp. 101 :13 – 24.

Catherine Kuhna, Aline de Matos Valeriob, Nick Ward, et al. 2019. Performance of Landsat-8 and Sentinel-2 surface reflectance products for river remote sensing retrievals of chlorophyll-a and turbidity. Remote Sensing of Environment, pp. 224:104–118

Chen J., Yin S.J., Xiao R.L.2014. Deriving remote sensing reflectance from turbid Case II waters using green-shortwave infrared bands based model.Advances in Space Research, pp. 53:1229-1238

Gallegos, C. L., Neale, P. J. 2002.Partitioning spectral absorption in case 2 waters: discrimination of dissolved and particulate components. Applied Optics, pp. 41(21): 4220 - 4233.

Gallie, E. A, Murtha, P. A. 1992.Specific absorption and backscattering spectra for suspended minerals and chlorophyll - a in Chilko Lake, British Columbia[J]. Remote Sensing of Environment, pp. 39 :103 - 118.

Han L H, Rundquist D C. The response of both surface reflectance and the underwater light field to various levels of suspended sediments: preliminary results. Photogrammetric Engineering & Remote Sensing, pp. 1994, 60 (12): 1463 - 1471.

Huang M.F, Xing X.F., Song Q.J., et al.2016. A new algorithm of retrieving petroleum substances absorption coefficient in seawater based on remote sensing image. Acta Oceanologica Sinica, pp. 35(11): 97-104.

Huang M.F., Song Q.J., Xing X.F., et al..2014a. Bio-optical model of retrieving petroleum concentration in sea water [J]. Acta Oceanologica Sinica, pp. 34(5):81-85

Huang, M.F., Song, Q.J. and Chen, L.B., 2015. Research on an inverse model of petroleum content in water bodies based on the normalized remote sensing reflectance. Journal of Ocean Technology, pp. 34 (1), pp. 1-9.

Huang, M.F., Song, Q.J., Jiang W. J. et al..2012. The retrieval model for petroleum concentration in waters using remote sensing data. Acta Oceanologica Sinica, pp. 34(5):74-80

Huang, M.F., Song, Q.J., Xing, X.F., et al. 2014b. Analysis of fluorescence spectrum of petroleum-polluted water. Spectroscopy and Spectral Analysis, pp. 34(9):2466-2471.

Huang, M.F., Wang D. F., Xing, X.F., et al..2015. The research on remote sensing mode of retrieving $a_g(440)$ in Zhujiang River Estuary and its application .Acta Oceanologica Sinica, pp. 37(5):66-77.

Huang, M.F., Xing, X.F., Song, Q.J., et al., 2017. New algorithms to separate the contribution of petroleum substances and suspended particulate matter on the scattering coefficient spectrum from mixed water. Spectroscopy and Spectral Analysis, pp. 37(1), pp. 205-211.

Jiang, G. J., Steven A. L., Yang D.T., et al. 2019. An absorption-specific approach to examining dynamics of particulate organic carbon from VIIRS observations in inland and coastal waters. Remote Sensing of Environment, pp. 224: 29-43

Lee, Z.P. & Carder K.L. .2004. Absorption spectrum of phytoplankton pigments derived from hyperspectral remote-sensing reflectance. Remote Sensing of Environment, pp. 89: 361 - 368.

Luba B.& Loise H. 2007. Variability and classification of remote sensing reflectance spectra in the eastern English Channel and southern North Sea. Remote Sensing of Environment, pp. 110 :45–58

Lyu H., Wang Q. Wu C.Q., et al.2013 Retrieval of phycocyanin concentration from remote-sensing reflectance using a semi-analytic model in eutrophic lakes[J]. Ecological Informatics 2013, pp. 18:178–187
Ma, R. H., Song Q. J., Tang J. W., et al.2007. Asimple empirical model for remote sensing reflectance of Lake Taihu waters in autumn. Journal of Lake Sciences, pp. 19(3):227-234
Martin Ligi, Tiit Kutser, Kari Kallio.2017. Testing the performance of empirical remote sensing algorithms in the Baltic Sea waters with modelled and in situ reflectance data. Oceanologia, pp. 59:57- 68.
Monika Soja-Woźniak, Mirosław Darecki, Bożena Wojtasiewic. 2018. Laboratory measurements of remote sensing reflectance of selected phytoplankton species from the Baltic Sea. Oceanologia, pp. 60:86-96.
Pope, M., Fry, E. S. 1997. Absorption spectrum (380 - 700nm) of pure water. II Integrating cavity measurements. Applied Optics, pp. 36(33): 8710 - 8723.
Shu X.Z., Wan G.F., Shen M.M,et al.2000. Remote Sensing of Water Quality Monitoring using an Airborne Imaging Spectrometer. pp. 19(4):273-276.
Sławomir B. Woźniak, Mirosław Darecki, Monika Zabłocka, et al. 2016. New simple statistical formulas for estimating surface concentrations of suspended particulate matter (SPM) and particulate organic carbon (POC) from remotesensing reflectance in the southern Baltic Sea. Oceanologia, pp. 58:161-175
Smith, R. C., Baker, K. S. 1981.Optical properties of the clearest natural waters (200 - 800nm) [J]1 Applied Optics, pp. 20: 177 - 1841.
Song, Q. J., Tang, J. W., 2006. The study on the scattering properties in the Huanghai Sea and East China Sea. Acta Oceanologica Sinica, 28(4), pp. 56-63.
Xing X.F, Xie S.Y. Huang M.F., et al. 2018. Characteristics of Biochemical Parameter and Its Correlation Analysisi in Chudao Island Seawater of Weihai City. JOURNAL OF OCEAN TECHNOLOGY, pp. 37(1):54-61
YIN L., TANG J.W., SONG Q.J. 2011. A method of classification for algal species based on remote sensing reflectance spectra. ACTA OCEANOLOGICA SINICA, pp. 33(3):55-62
Yu H. Cai Q.M., Wu J.L. 2003. Study on characteristic of the absorption and scattering coefficients of Taihu Lake waters. ADVANCES IN WATER SCIENCE, pp. 14(1):47-49.
Zhang M.W., Hu C.M., Cannizzaro J., et al. 2018. Diurnal changes of remote sensing reflectance over Chesapeake Bay: Observations from the Airborne Compact Atmospheric Mapper. Estuarine, Coastal and Shelf Science, pp. 200 :181-193